



Coupling by charge transfer: role in bond stabilization for open-shell systems and ionic molecules and in harpooning and proton attachment processes†

F. PIRANI¹, A. GIULIVI¹, D. CAPPELLETTI² and V. AQUILANTI^{1*}

¹ Istituto Nazionale per la Fisica della Materia (INFN) and Dipartimento di Chimica, Università di Perugia, 06100 Perugia, Italy

² Istituto Nazionale per la Fisica della Materia (INFN) and Sezione di Tecnologie Chimiche DICA, Università di Perugia, 06100 Perugia, Italy

(Received 8 March 2000; revised version accepted 28 April 2000)

A variety of phenomena of apparently different nature can be compacted and described within a unifying picture by taking into account the role of the charge transfer interaction. Relevant information on this interaction is obtained by the analysis of bond stabilization in halides, oxides, sulphides and ionic dimers of rare gases. Most of this information comes from recent molecular beam experiments: when combined with the analysis of processes occurring at crossings between covalent and ionic states in alkali halides it leads to the characterization of the dependence of the charge transfer matrix element on basic physical properties of the interacting partners. The magnitude of the coupling matrix element is correlated to polarizabilities and charges. Its exponential decreasing with intermolecular distance is given in terms of ionization potentials and electron affinities, in the spirit of the study by Grice and Herschbach (*Molec. Phys.*, 1973, **27**, 159) on the long-range configuration interaction of ionic and covalent states. A proper representation is obtained both for the transition from van der Waals to chemical bonds and for the behaviour of different families of compounds, such as those of alkali halides and of rare-gas protonated systems.

1. Introduction

We report a study of the role that the coupling by charge transfer plays in a variety of phenomena, and offer an assessment of its strength and dependence on the intermolecular distance. Some of the present results have been obtained by extending a methodology applied by Grice and Herschbach [1, 2] to the study of the phenomenology of the configuration interaction among neutral and ionic states. Our analysis also includes more recent experimental information.

The focus of our investigation is the characterization of the main interaction components of intermolecular potentials, in order to establish empirical relationships among their features (such as ranges and strengths, including dependences on intermolecular distance and mutual orientations) and fundamental physical properties of the interacting partners. This effort is not to be considered as alternative to, but as complementary to the development of the *ab-initio* and semiempirical

methods [3, 4] of quantum chemistry: it can be relevant both to insert within a unified framework an apparently sparse wide set of phenomena and to make reliable forecasts for the structure and dynamics of systems not immediately available to experimental and theoretical studies.

Our previous work along these lines has considered neutral–neutral [5], ion–neutral [6] and ion–ion [7] systems, interacting respectively with ‘pure van der Waals’, ‘van der Waals plus induction’ and ‘van der Waals plus induction and Coulombic’ forces. Correlation formulas have been proposed in terms of polarizability and charge of the individual partners, allowing a proper evaluation of the role of the various contributions to the overall interaction.

Crucially important is often the contribution of charge transfer, for which direct experimental information is limited. This component of the interaction is typically elusive to calculations. A full configuration interaction approach, unavoidable for an accurate treatment of this problem, involves typically many states and is a bottleneck of quantum chemistry: the recent developments of semiempirical (e.g. density functional theory) methods encounter here severe difficulties.

* Author for correspondence. e-mail: aquila@dyn.unipg.it

† This paper is dedicated to the memory of Professor Roger Grice (1941–1998).

A list of phenomena where charge transfer plays a role includes: harpooning reactions between metal atoms and molecules with high electron affinity [8, 9], ion-recombination processes leading to excited neutral products [10], ion-molecule reactions promoted by an electron exchange between reagents [11], Coulombic explosion induced by charge transfer within multiply ionized systems [12], bond stabilization in symmetric and asymmetric rare-gas ionic dimers [13–18] and in rare-gas oxides and halides [19–27], selectivity in chemical reactions induced by long-range forces [28], spectroscopic properties of excimers [29, 30], and collisional autoionization and excitation transfer occurring in collisions of metastable rare-gas atoms with other atoms or molecules [31].

The purpose of this work is to obtain information on charge transfer coupling, that is explicitly on the matrix element between two quantum states of the interacting complex which differ by the exchange of an electron. The present analysis, which focuses mainly on atom-atom and ion-atom systems, also takes into account some atom-molecule cases, with no explicit reference to molecular anisotropy.

Section 2 presents an ample phenomenology associated with charge transfer and its description in terms of two-state coupling. The role of charge transfer in the transition from van der Waals to chemical bond and at the crossing between ionic and covalent states is discussed in sections 3 and 4: a general correlation formula for the strength of the charge transfer coupling is introduced and tested. Relevance of this interaction component for proton affinity is analysed in section 5. Conclusions follow in section 6. The Appendix is devoted to the relationships between some commonly used spectroscopic constants and interaction potential parameters.

2. Charge transfer as an effective two-state problem

2.1. Phenomenology and role in bond stabilization

The quantum mechanical study of charge transfer effects requires the explicit treatment of configuration interaction among states of the same symmetry which differ for one-electron exchange. Within this manifold, the attention has often been focused upon those two states that are closest in energy and exhibit the strongest coupling. These states and their mutual interaction are conveniently described as a function of an effective variable R , which is the intermolecular distance for processes, such as those presently analysed, involving atom-atom systems or dominated by long-range forces. For molecular processes, R can be for example the hyper-radius, that is the nearly separable variable of hyperspherical treatments of elementary chemical reactions.

In order to rationalize a wide set of phenomena, promoted by charge transfer, we distinguish three cases.

(i) Non-resonant charge transfer (figure 1)

Examples are bond stabilization phenomena in rare-gas oxides and halides and in asymmetric rare-gas ionic dimers. Their importance increases as the intermolecular distance R and/or the energy separation $\Delta V(R) = |V_a(R) - V_b(R)|$ (V_a and V_b are ‘diabatic’ potentials referring to the two coupled states, see figure 1) decrease. A

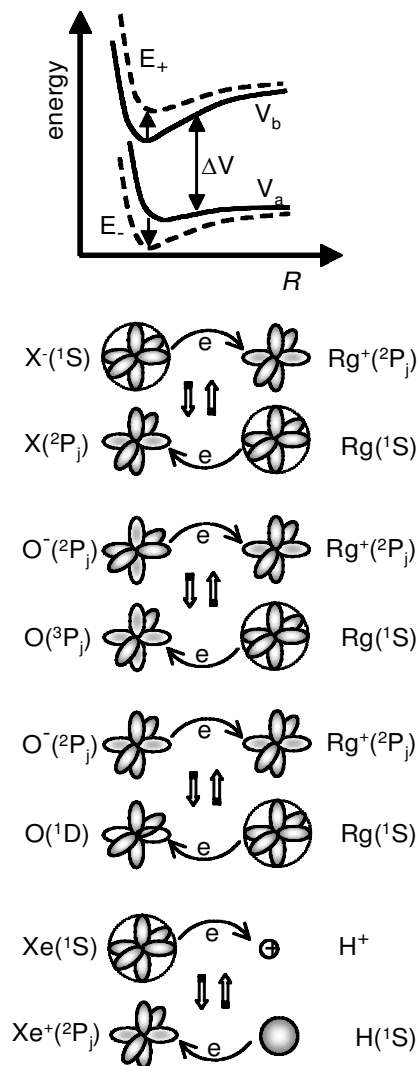


Figure 1. Examples of non-resonant charge transfer. V_a and V_b are diabatic interactions and E_+ and E_- are adiabatic energies. ΔV is the energy separation between the coupled states. The coupling stabilizes E_- with respect to V_a and destabilizes E_+ with respect to V_b . Filled, half-filled and empty orbitals are indicated by dark, medium and no shading. From top to bottom: the cases of rare-gas halides (the asymmetric rare-gas ionic dimers behave similarly), rare-gas oxides (with 3P oxygen atom), rare-gas oxides (with 1D oxygen atom) and the XeH^+ system.

further example, the proton affinity in cases such as that of the Xe atom, will be considered later (section 5).

(ii) *Charge transfer localized near degeneracy between two surfaces* (figure 2)

The phenomena promoted by this effect occur in the neighbourhood of diabatic crossings and their role depends on the strength of the coupling between the two states. The mechanisms of ‘harpooning’ in alkali halides, of dissociation in doubly ionized molecular systems and of proton attachment for the rare-gases (except Xe) belong to this class (see section 5).

(iii) *Resonant charge transfer* (figure 3)

The classic example is H_2^+ (section 4): in this case, electron transfer is operative at all R , although with a decreasing efficiency as R increases. Similar phenomena are active in symmetric rare-gas ionic dimers and in the collisional auto-

ionization of excited metastable atoms, which is assumed to occur mainly through an electron exchange mechanism [31].

Figures 1, 2 and 3 give a pictorial representation of some phenomena pertaining to cases (i), (ii) and (iii): they suggest their strong dependence on the intermolecular distance R and on the relative orientation of the valence orbitals involved in the exchange of the electron.

Within the framework of a quantum mechanical two-state problem, the potential energy is written in the following matrix form:

$$\begin{pmatrix} V_a(R) & \beta(R) \\ \beta(R) & V_b(R) \end{pmatrix}$$

where $V_a(R)$ and $V_b(R)$ are the diabatic interactions and $\beta(R)$ is the *coupling matrix element*—the target of this work. The eigenvalues $E_{\pm}(R)$ are the adiabatic energies,

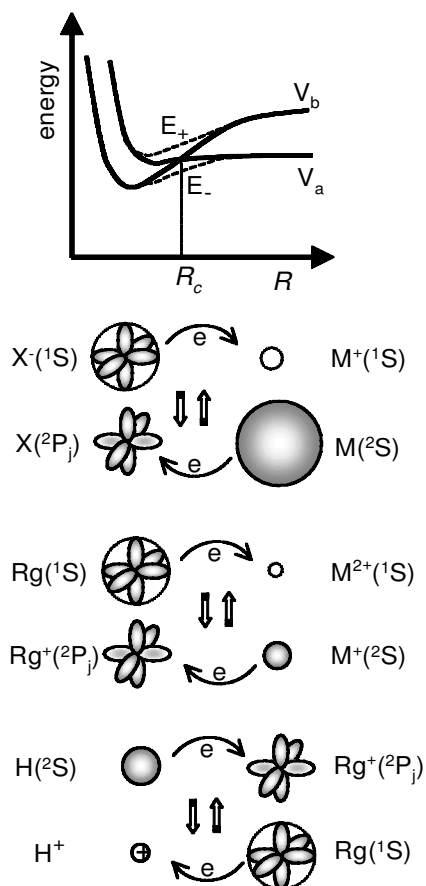


Figure 2. Examples of charge transfer localized near degeneracy between two surfaces (as in figure 1). The three examples here correspond to alkali halides, rare-earth-metal rare-gas dication and to the protonated rare gases (other than Xe).

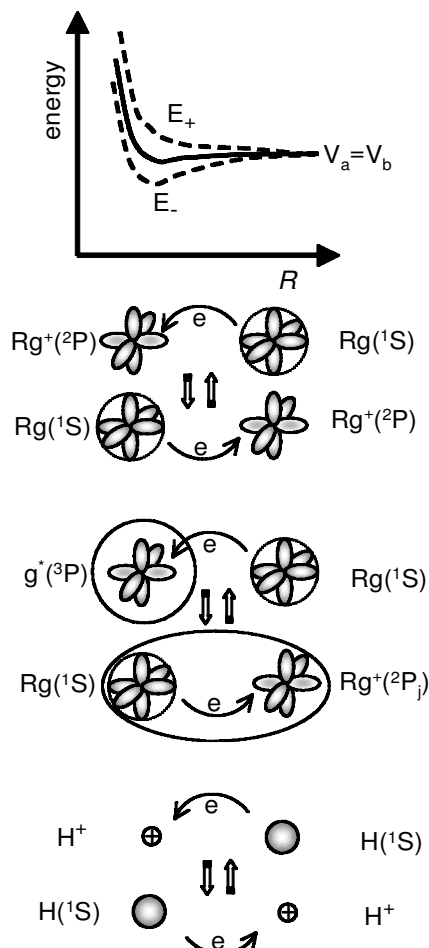


Figure 3. Examples of resonant charge transfer (as in figure 1) illustrating the cases of H_2^+ , of symmetric rare-gas dimer ions and systems giving autoionization processes, for which the circle and the ellipse represent the excited electron.

given by (omitting explicit reference to the R dependence):

$$E_{\pm} = \frac{V_a + V_b}{2} \pm \left[\left(\frac{\Delta V}{2} \right)^2 + \beta^2 \right]^{1/2},$$

where $\Delta V = |V_a - V_b|$. The *bond stabilization* V_x , introduced in [27], is explicitly related to the adiabatic splitting:

$$E_+ - E_- = 2 \left[\left(\frac{\Delta V}{2} \right)^2 + \beta^2 \right]^{1/2} = \Delta V + 2V_x, \quad (1)$$

namely

$$V_x = \left[\left(\frac{\Delta V}{2} \right)^2 + \beta^2 \right]^{1/2} - \frac{\Delta V}{2},$$

or

$$\beta^2 = V_x(V_x + \Delta V). \quad (2)$$

These relationships show that the contribution of the coupling β to the bond stabilization V_x is attenuated by the energy separation ΔV between the coupled states.

Two limiting cases of equation (2) are of interest. The case $\Delta V \gg V_x$, leading to:

$$V_x \simeq \frac{\beta^2}{\Delta V}, \quad (3)$$

is appropriate to describe most phenomena sketched in figure 1; the case $\Delta V \simeq 0$, that is

$$V_x \simeq \beta,$$

applies to most of the phenomena depicted in figures 2 and 3. Some relevant information on V_x has been provided by spectroscopic (see e.g. [32]) and scattering (see e.g. [21–25, 28]) studies. However, quantitative comparisons of theoretical predictions and experimental information on the coupling β are scarce and uncertain.

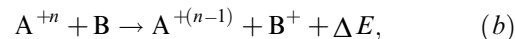
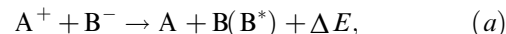
2.2. Factors influencing the coupling β

In the past, several attempts, essentially semiempirical in character, have been made to represent strength and R dependence of the coupling β , in terms of fundamental physical properties of the interacting partners. The purpose has been to find scaling laws sufficiently valid to compact data coming from existing information, and to allow extensions to systems not readily accessible to experiments or theory. An outline of the long history of these attempts is in order for a proper assessment of the developments proposed in this work.

Magee [33] first introduced the basic idea that β , at long range, is proportional to the overlap integral S_{ij} of the transferred electron wavefunctions between i and j orbitals. On these grounds, Grice [1], studying the

asymptotic behaviour of wavefunctions, developed a simple treatment which clarifies the dependence of β on properties of the interacting partners.

Olson *et al.* [34], reviewing previous work [35, 36] on some processes illustrated in figure 2, namely



gave arguments in favour of the representation of β as a decreasing exponential function of the crossing radius R_c :

$$\beta(R_c) = AR_c \exp(-\gamma R_c) \quad (4)$$

They proposed also the use of the following equation, in reduced variables, to correlate different systems (all quantities are in atomic units):

$$\beta^*(R_c) = A^* R_c^* \exp(-\gamma^* R_c^*), \quad (5)$$

where

$$\beta^*(R_c) = \frac{\beta(R_c)}{(I_1 I_2)^{1/2}}, \quad R_c^* = R_c \left(\frac{I_1^{1/2} + I_2^{1/2}}{2^{1/2}} \right) \quad (6)$$

In (6) I_1 is the ionization potential of the donor and I_2 is the electron affinity of the acceptor. For an ionic acceptor A^{+n} (see (b) above), I_2 corresponds to the ionization potential of $A^{+(n-1)}$. The coefficient γ^* was found to be close to 1 [2, 34], and thus it was suggested that γ , in (4), can be defined as

$$\gamma = \frac{I_1^{1/2} + I_2^{1/2}}{2^{1/2}}. \quad (7)$$

To permit a proper description of $\beta(R)$ in the long and intermediate range of R , a slightly modified version of (4) has been used in a subsequent work [37]:

$$\beta(R) = AR^m \exp(-\gamma R), \quad (8)$$

where the m parameter depends on I_1 and I_2 and γ is defined as in (7). Equation (8) has been adopted also in this work, as discussed in section 5.

Important progress towards a unifying picture of many processes of type (a) was made by Grice and Herschbach [2]. Their analysis, which included further data and was of higher accuracy with respect to previous attempts [34], led to the proposal of scaling laws and correlations, valid, however, only within given families (iodides, bromides, etc) (see also section 4). These authors suggested also that a more appropriate normalization procedure should take into account other properties of the acceptor partner, such as the atomic radius.

The analysis of the recently available phenomenology allows us to characterize the dependence of β on other fundamental physical properties besides the ionization

potential of the donor (I_1) and the electron affinity of the acceptor (I_2). In the following we shall show that the properties of S_{ij} (and β) at intermediate intermolecular distances also depend on the combined effect of repulsive and attractive forces, which are operative between the two partners in the absence of a pronounced deformation of the respective electronic clouds.

We have provided ample evidence ([38], see also [39]) that *size* effects, which determine the range for the onset of the repulsion, are correlated with polarizabilities of the two partners. Also defined in terms of polarizabilities and permanent charges are dispersion, induction and electrostatic forces [5–7].

In the next section we propose a formula that establishes a correlation between the coupling β and the specific features (strengths and ranges) of the interaction components of van der Waals, induction and electrostatic nature. These components—which do not include ‘chemical’ contributions, such as those due to electronic angular momenta couplings and charge exchange—will be given in terms of polarizabilities and permanent charges of both partners.

To achieve this, we have considered information as obtained from a systematic analysis of bond stabiliza-

tion by charge transfer in systems involving open-shell atoms with high electron affinity (see figure 1). In the rare-gas fluorides, chlorides and oxides, this information has been obtained empirically from molecular beam scattering experiments (see next section and [27]), carried out using the molecular beam technique coupled with velocity and state analysis [21–25, 28]. A recent paper [26] reports on experimental studies of rare-gas sulphides. The proposed relationships are analysed and tested against the salient features of other phenomena of the type depicted in figures 1–3.

3. The transition from van der Waals to chemical bonds

A proper framework to discuss the interactions in open-shell atom–closed-shell atom (or spherical molecules) has been established [40–43] to be in terms of isotropic component $V_0(R)$ and an anisotropy $V_2(R)$, which represents orbital alignment effects. Both these components are related simply, through angular momentum coupling analysis, to sums and differences of the familiar $V_\Sigma(R)$ and $V_\Pi(R)$ interactions (see figure 4). Relevant relationships are:

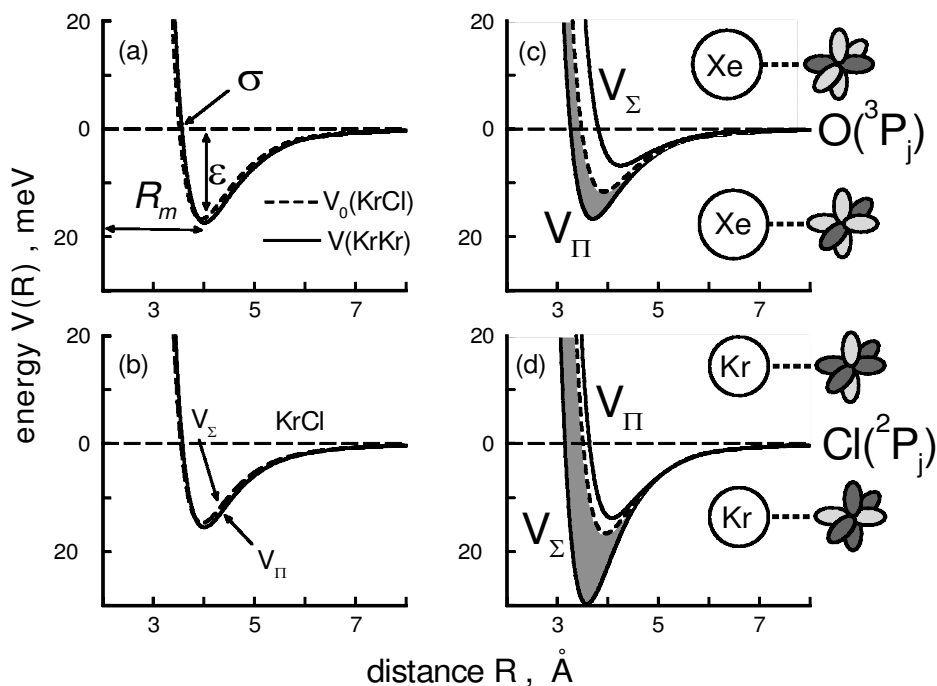


Figure 4. (a) The main features of a typical van der Waals interaction for the case of Kr_2 and the isotropic interaction $V_0(R)$ of KrCl for comparison (the open-shell Cl atom and Kr show a similar polarizability). (b) The isotropic interaction potential of KrCl of (a) is split into Σ and Π components by the Cl atom polarizability anisotropy only. Examples of open-shell interactions from experimental studies are reported for (c) XeO [21] and (d) KrCl [25]. Half-filled (grey) and filled (black) valence orbitals of Cl and O atoms are also sketched. (---) The spherical component and (—) the $V_\Sigma(R)$ and $V_\Pi(R)$ interactions, which correspond to the different symmetries of the molecular orbitals. The effect of the bond stabilization energy V_x is depicted by the shaded areas in (c) and (d).

$$V_0 = \frac{(V_\Sigma + 2V_\Pi)}{3} \quad V_2 = \frac{5(V_\Sigma - V_\Pi)}{3},$$

or inversely

$$V_\Sigma = V_0 + \frac{2}{5}V_2 \quad V_\Pi = V_0 - \frac{1}{5}V_2.$$

This representation is suitable for the analysis of scattering results. Its usefulness is appreciated also from the fact that a thorough analysis of the data on the $V_0(R)$ interaction leads to definition of its nature in terms of van der Waals forces. Indeed, the potential energy features ϵ , R_m and σ (see figure 4(a)), which represent respectively the bond strength, the equilibrium distance and the zero value of $V_0(R)$ interaction, agree with the predictions of correlation formulas [5] involving only the polarizabilities of the interacting partners.

The $V_2(R)$ component of the interaction can be immediately related with the bond stabilization energy $V_x(R)$:

$$V_x = \frac{2}{5}|V_2| = \pm(V_0 - V_\Sigma).$$

The sign (e.g. minus for oxides and plus for halides) depends on the orientation of atomic valence orbitals which lead to molecular states with a specific symmetry (see figure 4). The main effect of $V_2(R)$ is therefore the removal of the degeneracy in $V_0(R)$. Experimentally determined bond stabilizations $V_x(R)$ regularly increase along homologous series, according to the decrease of the ionization potential of the closed-shell partner [21–28]. Indeed they are found to be too large to be attributed solely to anisotropy of the van der Waals components. In particular, figure 4(b) shows that the polarizability anisotropy of the open-shell atom (Cl in this case) is generally too small to account for the observed effects, which are especially large when heavier partners are involved (such as Kr and Xe, 4(c) and (d)).

Therefore, for systems that contain an open-shell atom with high electron affinity, charge transfer contributions to the potential energy, due to a configuration interaction among the lowest neutral and higher ionic molecular states of the same symmetry (which differ for an electron exchange), substantially contribute to $V_2(R)$, and thus to the stabilization of the bond. For rare-gas halides, these contributions are relevant essentially in the Σ symmetry, because this involves a larger probability of electron exchange (see figure 4(d)). Explicitly,

$$V_x = V_0 - V_\Sigma.$$

For oxides and sulphides (figure 4(c)) this applies to the Π symmetry, and we have

$$V_x = 2(V_0 - V_\Pi) = V_\Sigma - V_0.$$

As seen in section 2, the bond stabilization V_x depends also on the energy separation between the interacting states. This dependence establishes the key connection

with the experimental observation [21–26, 28] of the increase of V_x along a homologous series, corresponding with the decrease of the ionization potential of the closed-shell partner.

For the following discussion, in order to compare different systems, we consider $R = \sigma$ (see figure 4(a) and [27]) as the proper reference distance, where attractive and repulsive components of $V_0(R)$ balance:

$$V_0(\sigma) = V_{\text{attraction}}(\sigma) + V_{\text{repulsion}}(\sigma) = 0. \quad (9)$$

Moreover, at σ experimental data provide direct information on V_2 and V_x . Specifically, for fluorides and chlorides

$$V_x(\sigma) = -V_\Sigma(\sigma),$$

while for oxides and sulphides

$$V_x(\sigma) = -2V_\Pi(\sigma) = V_\Sigma(\sigma).$$

Experimental data on V_x [21–25, 28] suggest a direct proportionality on the attraction and an inverse dependence on ΔV , the energy separation (section 2) between the states that are coupled by charge transfer:

$$V_x(\sigma) \propto \frac{V_{\text{attraction}}(\sigma)}{\Delta V(\sigma)}. \quad (10)$$

Figure 5 illustrates correlation (10) for the cases of oxides [21, 22] and chlorides [25, 28]. Since the attraction scales linearly with ϵ (the bond strength of the V_0 component, see figure 4(a)) [7], this result is in accord with the previously proposed empirical formula [27]

$$V_x(\sigma) = \frac{k\epsilon}{\Delta V(\sigma)}, \quad (11)$$

where $k = 16$ eV. The comparison of (11) with (3) suggests a phenomenological proportionality between $\beta^2(\sigma)$ and the bond strength ϵ of the spherical component V_0 of the interaction.

Empirical relationships (10) and (11) establish a proportionality between S_{ij}^2 (which defines β^2) and the sum over the squares of the overlaps of all valence orbitals in the unperturbed systems, S^2 . For cases involving atoms with high electron affinities (such as halogens, oxygen and sulphur) this is a consequence of the fact that the outer electronic distributions are only slightly modified when negative ions are formed [2]. Also, since the repulsion energy is proportional to S^2 [44, 45] and, at σ , repulsion and attraction balance (equation (9)), the following proportionality relationship holds:

$$\beta^2(\sigma) \propto S_{ij}^2(\sigma) \propto S^2(\sigma) \propto V_{\text{attraction}}(\sigma) \propto \epsilon \quad (12)$$

Figure 6 illustrates for neutral–neutral systems the connection of β with the σ and ϵ potential features, which depend on the polarizabilities of the partners [5]. For

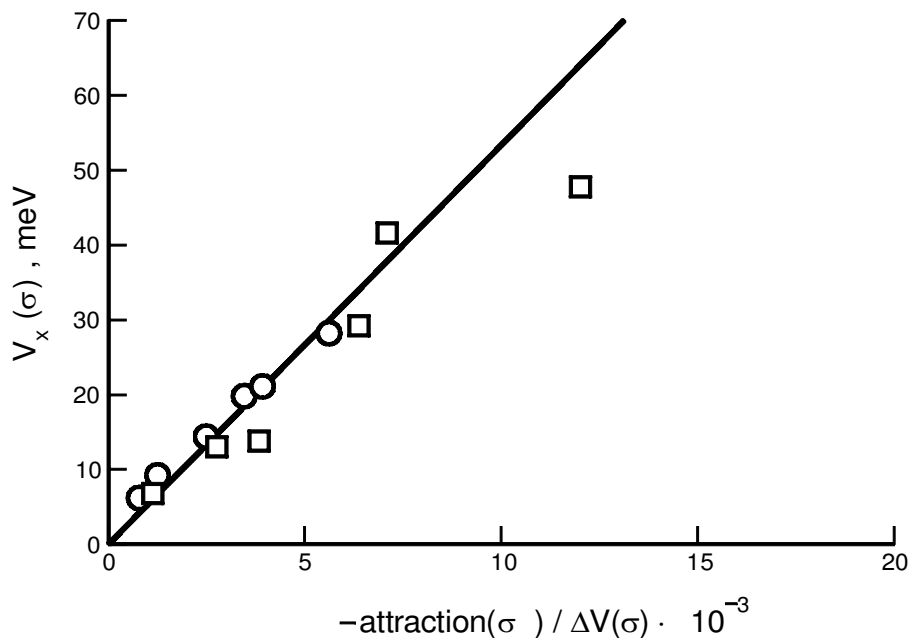


Figure 5. Bond stabilization energies V_x as a function of the ratio between $V_{\text{attraction}}$ and ΔV (equation 10) at the reference distance σ . $\Delta V(\sigma) \simeq I_1 - I_2 - 14.4/\sigma$ when energies are in electronvolts and distances in ångströms (see e.g. [8]). Circles and squares are experimental data from [21, 22, 25, 28]. The line represents the behaviour, in the limit of $\Delta V \gg V_x$, of a general correlation (equation (13)), obtained by the analysis of several other systems (see text and figure 7).

systems involving ions, the dependence on the charge must be included, as in [6, 7].

The proper combination of equation (2) with the empirical relationship (11) leads to the following correlation formula:

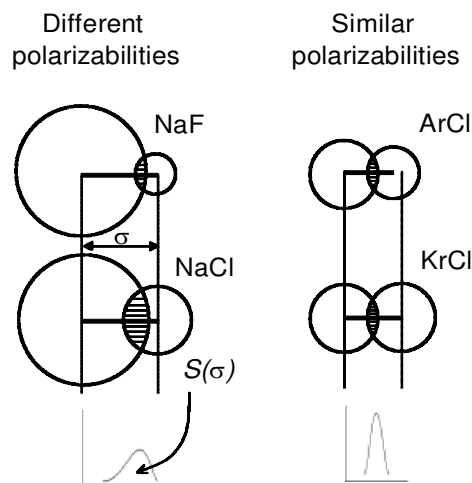
$$\beta^2(\sigma) = V_x(\sigma)(V_x(\sigma) + \Delta V(\sigma)) = k\epsilon, \quad (13)$$

which is of relevance because it relates the coupling $\beta(\sigma)$ and the bond stabilization $V_x(\sigma)$ with the bond strength of V_0 and the energy separation $\Delta V(\sigma)$ between the coupled states.

A test of the validity of equation (13) is shown in figure 7 which includes not only chlorides and oxides, but also fluorides, bromides, iodides, sulphides and the rare-gas dimer ions (both symmetric and asymmetric).

This empirical correlation formula allows us to discuss, for this set of weakly bound molecules, the transition from van der Waals to chemical bonds. Specifically the NeO system, reported in figure 7, has $\epsilon \simeq 4$ meV and $\Delta V(\sigma) = 15.2$ eV: $\beta(\sigma)$ is small and its effect, strongly attenuated by $\Delta V(\sigma)$, provides $V_x(\sigma) \simeq 0$ indicating that the bond is nearly pure van der Waals. A similar behaviour can be ascribed to all open-shell atom–helium cases and most of the open-shell atom–neon systems. In Ar_2^+ , ϵ is larger ($\simeq 116$ meV) and $\Delta V(\sigma) = 0$: $\beta(\sigma)$ is also large and not attenuated by $\Delta V(\sigma)$, yielding a pronounced bond stabilization $V_x(\sigma)$, corresponding to the formation of a one-electron chemical bond. An intermediate behaviour is operative in systems as XeCl , XeF and NeAr^+ .

Figure 6. Illustration of the relationships among polarizabilities and the total orbital overlap S , at the characteristic distance σ , where attraction and repulsion balance (equation (9) and figure 4). Polarizabilities are responsible both for the strength of the attractive forces and for the proper scale of atomic sizes [38, 39]. The coupling β is known to be proportional to the overlap S_{ij} [33, 45] between the initial i and final j orbitals of the transferred electron. Since S_{ij} is proportional to S , and $S^2(\sigma)$ is proportional to the bond strength ϵ (see equation (12) and figure 4), a correlation holds between $\beta^2(\sigma)$ and ϵ (equation (13)). The R dependence of S is markedly influenced by features of the asymptotic behaviour of radial wavefunctions. Left: for partners of different polarizabilities (i.e. NaF and NaCl) σ depends on the size of the larger partner (higher polarizability) while $S(\sigma)$ depends mainly on the size of the smaller partner (lower polarizability). Right: for partners of similar sizes (i.e. ArCl and KrCl) $S(\sigma)$ and σ depend on the polarizabilities of both partners.



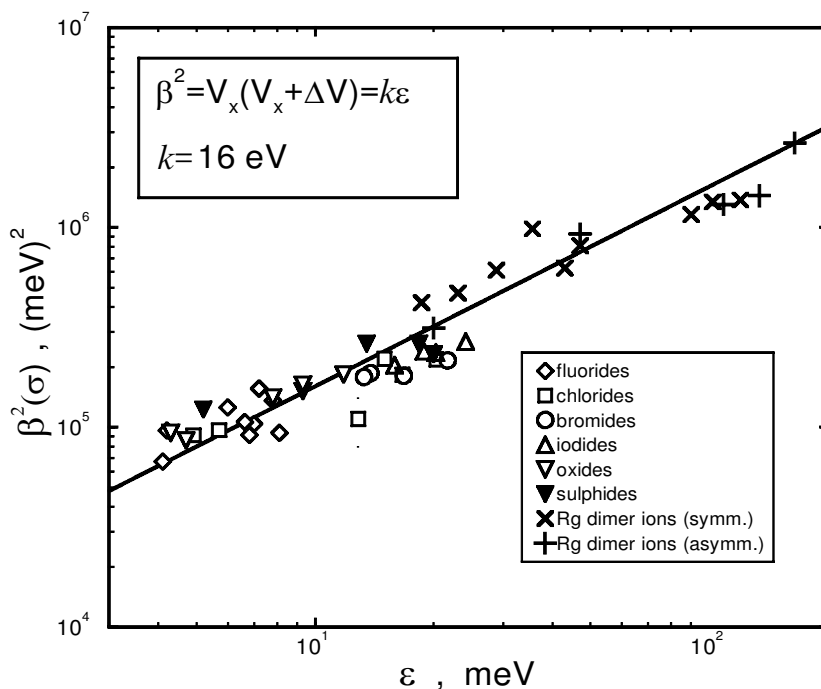


Figure 7. Correlation between $\beta^2(\sigma)$, obtained from experimental bond stabilization energies V_x and from known energy separations $\Delta V(\sigma)$, and the strength ϵ of the V_0 component of the interaction, for oxides, fluorides and chlorides [27]. The correlation formula $\beta^2 = k\epsilon$ (equation (13)) is represented by the continuous line. The figure shows that it can extend to data (mainly empirical) for symmetric and asymmetric rare-gas ion dimers [13–18] and rare-gas sulphides [26], bromides and iodides [19, 20].

4. The charge transfer coupling at crossings between ionic and covalent states

The alkali halides MX feature ionic and covalent states of the same symmetry which cross at a definite distance R_c (see figure 2). The coupling between the two states, due to charge transfer, gives a maximum effect at R_c ($\Delta V(R_c) = 0$).

A further test of the proposed correlation formula (13) involves the prediction of $\beta(\sigma)$ for such systems. The ϵ and σ values can be estimated empirically [5–7, 46] and the scaling procedures, equation (6), are considered valid also at σ . The predicted $\beta(\sigma)$ values for the potassium halides KX are reported in figure 8 together with those obtained by Grice and Herschbach [2] for

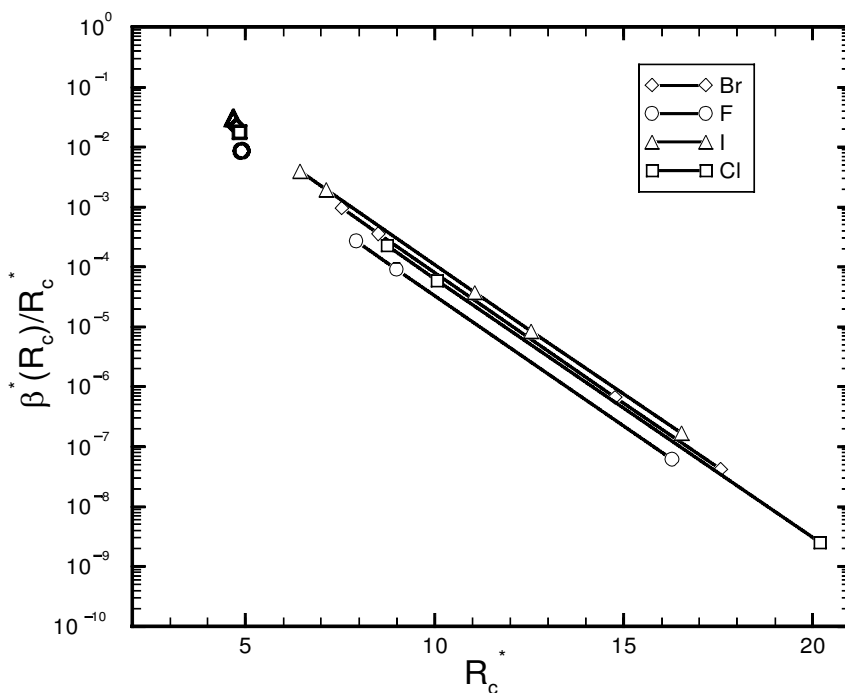


Figure 8. Ratios between the reduced quantity $\beta^*(R_c)$ and the reported reduced crossing distance R_c^* (equation (6)) reported versus R_c^* on a semilogarithmic plot for the alkali fluorides, chlorides, bromides and iodides. Straight lines are from [2] (see text). The isolated heavier symbols on the top left corner of the figure are predictions by the present work.

various families at larger intermolecular distances. For the other metals the predictions are found to correspond to the same reduced distance and would overlap with data shown in the figure.

The short distance extrapolation of the behaviour of each family, given by Grice and Herschbach [2], is qualitatively in agreement with the present results, which are consistently slightly higher. Note that the functional forms for $\beta(R)$ were suggested in [2] for large R , and that we are stretching their predictive power down to shorter distances. Also, spin-orbit effects, not included here, can be a further cause for a reduction of the $\beta(R)$ value [2].

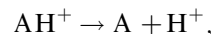
This analysis suggests that a better scaling of the β strength is by $\epsilon^{1/2}$, rather than by $(I_1 I_2)^{1/2}$ as in (6). Since for the alkali halides the ϵ value varies according to the polarizabilities of the halogen partner only [5, 46] (see also figure 6), a general interpolation relationship for these systems is

$$\beta^*(R_c) = \frac{\beta(R_c)}{(\alpha_2)^{1/2}} = 0.10 R_c^* \exp(-R_c^*), \quad (14)$$

where α_2 is the polarizability of the acceptor, and R_c^* is as in (6). This new scaling leads to the results plotted in figure 9, where other families of alkali metals interacting with oxygen and halogen molecules are included. The figure shows a universal plot for all families, spanning over several orders of magnitude and a wide intermolecular distance range.

5. Charge transfer and proton affinity

The proton affinity of an atom A, that is the energetics for the process



measures the binding energy of the proton to the atom A. The simplest system, to which we refer preliminarily, is that of the H atom, whose proton affinity corresponds to the binding energy for H_2^+ , for which accurate experimental and theoretical results are available. Further prototypical cases of interest are those of the rare-gas atoms, for which the molecular ions AH^+ are isoelectronic with hydrogen halides HX. Note, however, that the proton affinity of the rare-gases shows an opposite trend along the series with respect to the binding energy in the corresponding HX: the HF molecule exhibits the most stable bond while the proton affinity is highest for Xe [47].

Our point of view considers the ground state of AH^+ as resulting from the interaction between two limiting configurations of the same symmetry ($A \cdots H^+$ and $A^+ \cdots H$) which differ, at any R , for the exchange of one electron. Therefore the study of protonated systems such as HeH^+ , NeH^+ , ArH^+ and KrH^+ , for which the interactions in the diabatic and adiabatic representations are known with enough accuracy, can provide further details on the behaviour of the $\beta(R)$ coupling. This information will be used to predict value of proton affinity in other cases ($A = Xe, F, Cl$).

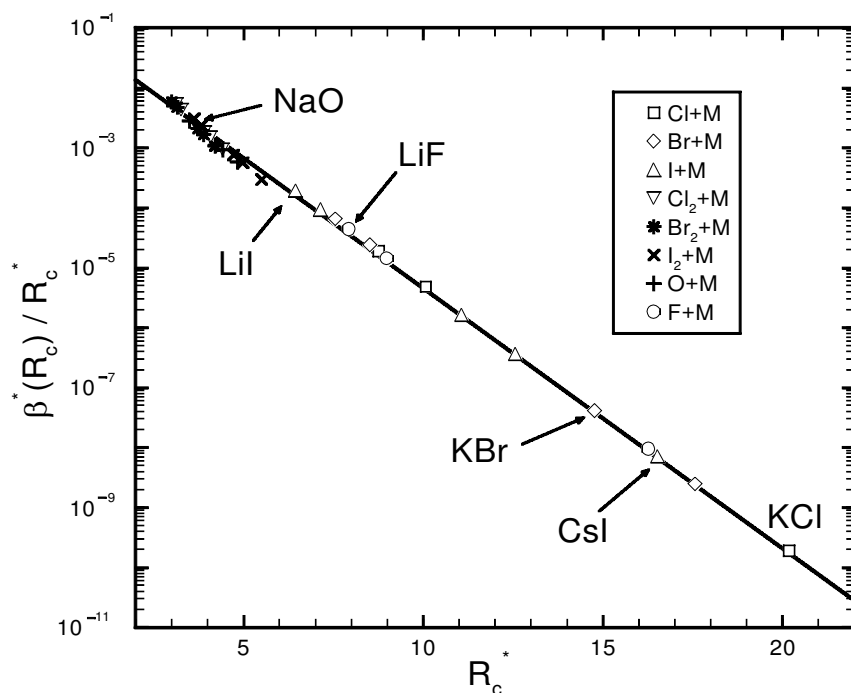


Figure 9. Ratios between the reduced quantity $\beta^*(R_c)$ (equation (14)) and the reported reduced crossing distance R_c^* (equation (6)) versus R_c^* on a semilogarithmic plot. The straight line is equation (14). The data are those in similar plots in [2] (see text) and [46]. With respect to the scaling procedure proposed in [46], formula (14) is seen to be simpler and the plot shows that the fitting power is comparable.

Specifically, in the case of $A = \text{He, Ne, Ar}$ and Kr relevant information on the adiabatic potential energy curve E_- (see figure 2) derives from spectroscopic and scattering studies (see Appendix) while reasonable predictions can be made on the ‘diabatic’ states V_a and V_b , respectively the $A \cdots \text{H}^+$ and the $A^+ \cdots \text{H}$ interactions. In this analysis V_b has been taken to be coincident with the potential curve of the $X(^1\Sigma)$ state of the isoelectronic HX molecule (in HeH^+ the reference molecule is H_2), while V_a has been considered as a point charge-neutral atom potential. The relationships between spectroscopic constants and intermolecular potential parameters, given in the Appendix, will be used for a suitable representation of the interactions.

5.1. The H_2^+ molecule as a test case

For this system the wavefunctions of the two coupled states asymptotically coincide with those of the LCAO method, and E_+ and E_- (see figure 3) correspond to the energies E_g and E_u of the *gerade* $^2\Sigma_g^+$ and *ungerade* $^2\Sigma_u^+$ molecular states. E_g and E_u can be combined to give:

$$\bar{E} = \frac{E_g + E_u}{2} \quad \text{and} \quad \beta = \frac{E_u - E_g}{2}.$$

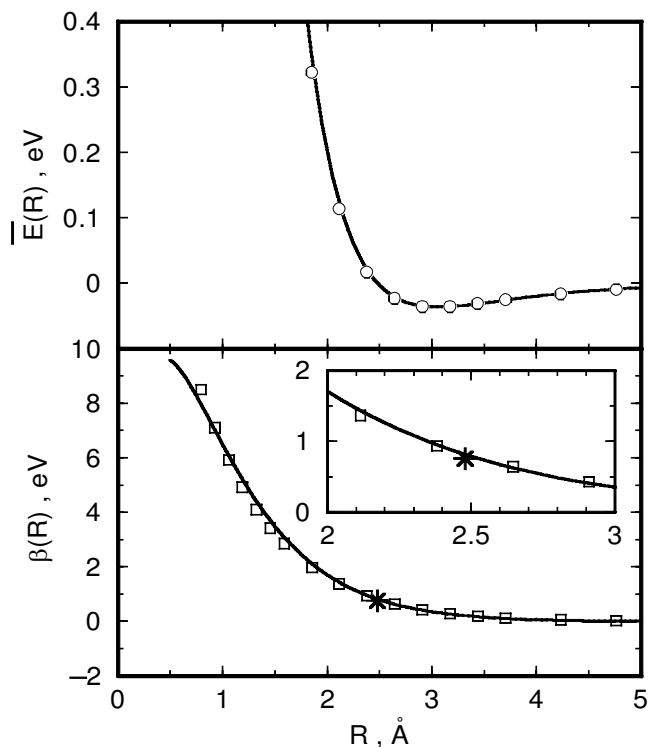


Figure 10. Open symbols are $\bar{E}(R)$ and $\beta(R)$ for H_2^+ (see section 5). Continuous curves are the best fit functions used in the present work. The star symbols represent the prediction of correlation formula (equation (13)).

Values for \bar{E} and β , obtained by exactly calculated E_g and E_u [48], are reported as circles in figure 10, where continuous lines represent the best fit of the data. We used a Morse function for \bar{E} to obtain the relevant ϵ and σ values. An exponential function (equation (8)) has been adopted for $\beta(R)$. In this case $\gamma = 1.0$ ($\text{au})^{-1} = 1.890 \text{ \AA}^{-1}$ has been fixed according to equation (7) while the best fit values obtained for A and m parameters are 43 (eV \AA^{-m}) and 0.800 respectively.

The value for $\beta(\sigma)$, predicted by the correlation formula (13), is also shown in figure 10. This important test encourages the application of equation 8 in a wide R range for the AH^+ systems.

5.2. The AH^+ systems

The potential energy curve $E_-(R)$ for HeH^+ , NeH^+ , ArH^+ and KrH^+ has been obtained following the procedure discussed in the Appendix. For the same systems, $V_b(R)$ has been derived analogously, making use of the spectroscopic constants of H_2 , HF , HCl and HBr in their ground state $X^1\Sigma$. The potential $V_a(R)$ has been estimated considering the proton-atom interaction, as determined by a combination of an attraction of the ion-multipole type and a repulsion due to the penetration of the proton in the outer electronic shell of the rare-gas atom. Results for E_- , V_a and V_b are shown in figure 11, while values of $\beta(R)$, derived by inverting equation (1), are plotted in figure 12, where the shaded areas define the range of $\beta(R)$ as determined by taking into account the uncertainty coming mainly from the repulsive part of V_a .

The results for $\beta(R)$ are compared in figure 12 with predictions (full lines) from equation (8), obtained with the procedure outlined in the following. The γ parameter has been fixed according to equation (7) (for ionization potential data see [47]). The m value has been calculated, in each case, from the empirical relationship

$$m = 0.566 I_A^{-1/2}$$

with I_A in atomic units. The numerical coefficient 0.566 has been chosen to agree with the value for m found for H_2^+ (see above). The coefficient A has been determined by imposing $\beta(R)$ to satisfy the general correlation for charge transfer given in equation (13). The required ϵ and σ values, reported in table 1 together with the predicted $\beta(\sigma)$, refer to the isotropic interaction component of the unperturbed $A^+ \cdots \text{H}$ state, and have been obtained by correlation formulas from [6, 7]. The choice of such reference states stems from the isoelectronicity of A^+ ions with halogen atoms, for which the procedure has been found to be adequate (see section 4). The A , m and γ parameters so obtained are reported in

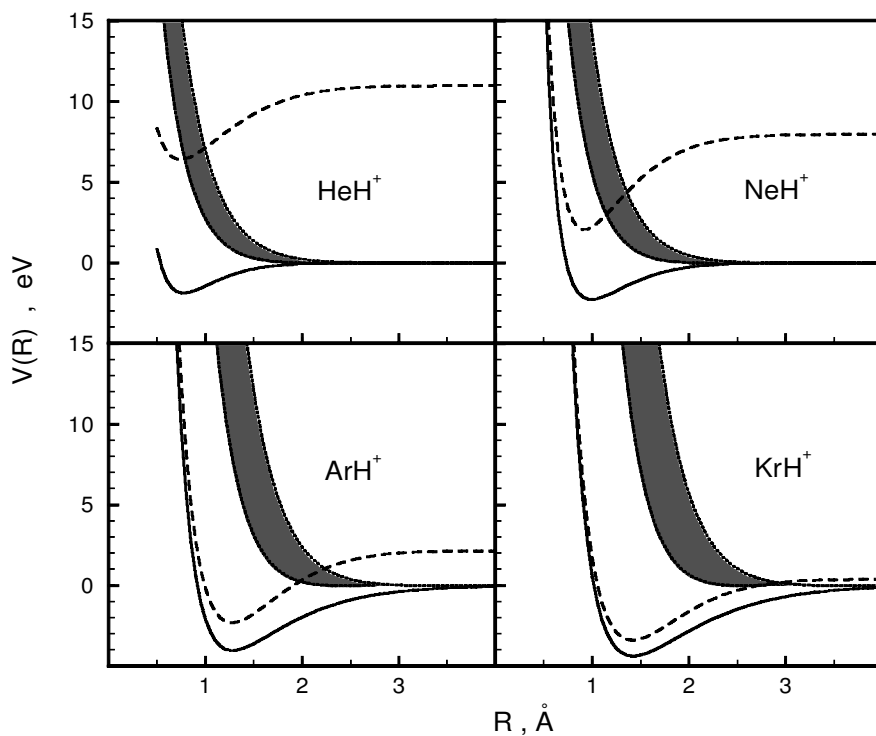


Figure 11. $E_-(R)$ (—, adiabatic energies), $V_a(R)$ (....., diatomic $H^+ \cdots A$ interactions) and $V_b(R)$ (---, diatomic $A^+ \cdots H$ interactions) for the AH^+ systems. The shaded areas represent the uncertainties associated with the $V_a(R)$ potentials.

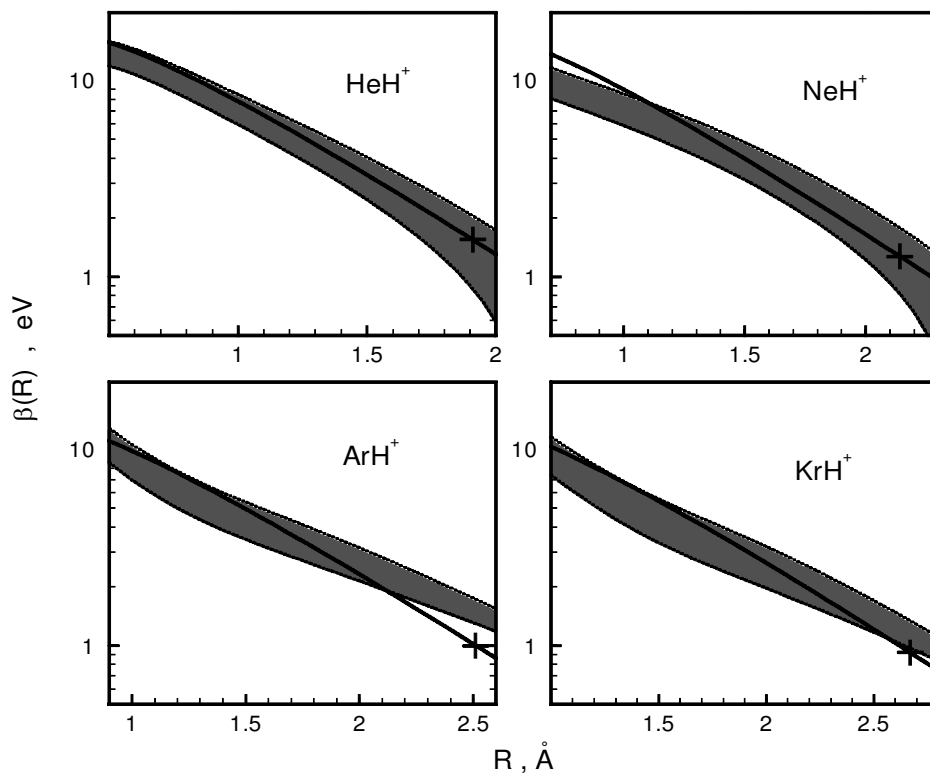


Figure 12. $\beta(R)$ values obtained from data of figure 11 (see text), with estimated uncertainties represented by the shaded areas. The crosses are the values obtained from the correlation formula (equation (13)) while solid lines are the present prediction $\beta(R)$ (see equation (8) and table 2).

table 2. In tables 1 and 2 are also given potential features and the A , m and γ parameters for XeH^+ , FH^+ and ClH^+ .

The coupling $\beta(R)$ has been used together with $V_b(R)$, obtained from spectroscopic constants of HI, HS and OH, and estimated $V_a(R)$ potentials, to predict the proton affinity in such cases. Predictions are compared with experimental values in table 3.

6. Conclusions

The present study has been focused on the role of the charge transfer interaction in several relevant physico-chemical phenomena. Our effort permits us to compact and to describe, into a unifying picture, processes of apparently different nature and allows us to obtain accurate information on the matrix element that describes the coupling between states which differ for the exchange of one electron.

Table 1. Bond strength ϵ , zero of the potential σ and coupling $\beta(\sigma)$ for the $\text{A}^+\text{-H}$ interaction.

System	ϵ (meV) ^a	σ (Å) ^a	$\beta(\sigma) = \sqrt{k\epsilon}$ (eV) ^b
He^+H	148	1.91	1.54
Ne^+H	100	2.14	1.27
Ar^+H	63	2.51	1.00
Kr^+H	53	2.67	0.92
Xe^+H	45	2.86	0.85
F^+H	88	2.24	1.19
Cl^+H	54	2.66	0.93

^aCalculated as in [7]. Polarizabilities are from [49] for H and from [7] for the rare gas ions. Estimated values (as in [37]) for F^+ and Cl^+ are 0.23 and 1.1 \AA^3 respectively.

^b $k = 16 \text{ eV}$, see section 3.

Table 2. Parameters used in equation 8 to calculate the coupling $\beta(R)$.

System	A (eV Å ^{-m})	m	γ (Å ⁻¹)
He^+H	71.3	0.597	2.210
Ne^+H	76.2	0.637	2.140
Ar^+H	70.0	0.746	1.966
Kr^+H	69.2	0.791	1.909
Xe^+H	66.4	0.850	1.836
F^+H	61.2	0.709	2.014
Cl^+H	59.7	0.822	1.867

Table 3. Comparison between predicted and available of proton affinities (eV).

System	Reference [47]	Present work
FH^+	3.4	3.8 ± 0.8
ClH^+	5.3	5.4 ± 0.5
XeH^+	5.1	5.4 ± 0.5

In the present analysis, an account has been given of: (i) the bond stabilization in systems involving open-shell atoms with high electron affinity, such as in rare-gas oxides, sulphides and halides; (ii) processes occurring at the crossing between covalent and ionic states; and (iii) the proton affinity in the rare-gas family.

This study leads to a representation of the coupling β in terms of fundamental physical properties of the interacting partners: the ionization potential of the donor and the electron affinity of the acceptor are responsible for the dependence of β on intermolecular distance R , while polarizabilities and charges determine its strength at the characteristic distance σ .

An empirical correlation (equation 13) has been introduced, which permits both a proper representation of the transition from van der Waals to chemical bonds and a rationalization of the behaviour of the coupling β in different families, such as those of the alkali halides and rare-gas protonated systems.

Further progress along these lines concerns the study of the dependence of charge transfer on the mutual orientation of the two partners, in order to understand the nature and role of steric effects in elementary chemical processes.

We acknowledge the support from the EU through the programme Training and Mobility of Researchers' Network 'Potential Energy Surfaces for Molecular Spectroscopy and Dynamics' (contract no. ERB-FMRX-CT96-0088). This work is also supported by the Ministero dell'Università e della Ricerca Scientifica e Tecnologica (MURST), by the Ente per le Nuove Tecnologie, l'Energia e l'Ambiente (ENEA), by the EU through the COST D9 Action and by the Istituto Nazionale di Fisica della Materia (INFN), Sezione A, through the PAIS 1999 project 'Dynamics of Charge-Transfer Processes'.

Appendix

Connection between interaction potential parameters and spectroscopic constants

According to Dunham [50] the effective potential V_{eff} of a vibrating rotor is represented as a series expansion

$$\begin{aligned}
 V_{\text{eff}} = & -\epsilon + a_0(x-1)^2 \left[1 + a_1(x-1) + a_2(x-1)^2 + \dots \right] \\
 & + B_e J(J+1) \left[1 - 2(x-1) + 3(x-1)^2 \right. \\
 & \left. - 4(x-1)^3 + \dots \right], \quad (16)
 \end{aligned}$$

where ϵ is the dissociation energy and B_e is the rotational constant at the equilibrium distance R_m and $x = R/R_m$. The first two terms define the interaction potential V , while the last term represents the contribution associated with the centrifugal force of rotation.

This treatment leads to the following expression for the energy levels of the vibrating rotor in the form (here the zero for the energy scale is taken at R_m)

$$F_{\nu,J} = \sum_{\ell,K} \mathcal{Y}_{\ell,K} \left(\nu + \frac{1}{2} \right)^\ell [J(J+1)]^K,$$

where ℓ and K are summation indices, ν and J are respectively vibrational and rotational quantum numbers, and $\mathcal{Y}_{\ell,K}$ are coefficients which depend on molecular constants.

Dunham [50] showed how the $\mathcal{Y}_{\ell,K}$ can be defined in terms of the a_i coefficients of the V expansion. The relationships involved simplify if the ratio between the rotational constant B_e and the frequency ω_e of small oscillations is much less than unity (all spectroscopic quantities being given as wave numbers). The $\mathcal{Y}_{\ell,K}$ terms also can be related to the ordinary band spectrum constants, taking into account the well known expansion of the molecular energy levels [51]:

$$F_{\nu,J} = \omega_e \left(\nu + \frac{1}{2} \right) - \omega_e x_e \left(\nu + \frac{1}{2} \right)^2 + \omega_e y_e \left(\nu + \frac{1}{2} \right)^3 + \dots \\ + B_\nu J(J+1) + \dots,$$

with $B_\nu = B_e - \alpha_e \left(\nu + \frac{1}{2} \right) + \gamma_e \left(\nu + \frac{1}{2} \right)^2$. Here the first term refers to a harmonic vibrator while the second and the third terms are anharmonic corrections. The α_e and γ_e constants correct the rigid rotor motion for the centrifugal stretching. Direct relationships among both a_i coefficients and potential derivatives around $x = 1$, and spectroscopic constants can be easily obtained.

The Dunham expansion is appropriate to represent the negative portion of the potential V around the minimum but it appears inadequate to describe other regions of the interaction, such as the repulsion at short range. Of interest here is a representation sufficiently reliable, also far from equilibrium distance.

A modified Morse function

$$V(R) = \epsilon [X^2 - 2X] \quad (A1)$$

where

$$X = x^{-a} \exp \left[b(1-x) + \frac{c}{2}(1-x^2) \right]$$

has been found suitable to describe both spectroscopic and high energy scattering properties in proton-rare-gas systems [52]. We have chosen this functional form since it is also reliable in the repulsion region.

The a , b and c coefficients have been found by imposing that at R_m second, third and fourth derivatives of the modified Morse function must be equal to those of a Dunham expansion potential, cut off at the fourth terms. The following relationships between a , b and c and spectroscopic constants are thus obtained:

$$R_m^2 V^{(2)} = 2\epsilon(a+b+c)^2 = \frac{2\omega_e^2}{4B_e},$$

$$R_m^3 V^{(3)} = -6\epsilon(a+b+c)^3 - 6\epsilon(a-c)(a+b+c) \\ = -\frac{6\omega_e^2}{4B_e} \left(\frac{\alpha_e \omega_e}{6B_e^2} + 1 \right),$$

$$R_m^4 V^{(4)} = 14\epsilon(a+b+c)^4 + 36\epsilon(a-c)(a+b+c)^2 \\ + 6\epsilon(a-c)^2 + 16\epsilon a(a+b+c) \\ = \frac{24\omega_e^2}{4B_e} \left[\frac{5}{4} \left(\frac{\alpha_e \omega_e}{6B_e^2} + 1 \right)^2 - \frac{2\gamma_e \omega_e}{3B_e} \right],$$

where $V^{(i)}$ are i th-order derivatives of V with respect to R in R_m , while $R_m^i V^{(i)}$ are the derivatives with respect to x .

Dissociation energies ϵ , bond lengths R_m and spectroscopic constants have been taken from [53], except those for NeH^+ [52, 54], ArH^+ [52, 55] and KrH^+ [52, 55].

References

- [1] GRICE, R., 1967, Ph.D. Thesis, Harvard University.
- [2] GRICE, R., and HERSCHBACH, D. R., 1974, *Molec. Phys.*, **27**, 159.
- [3] See for instance TANG, K. T., and TOENNIES, J. P., 1984, *J. chem. Phys.*, **80**, 3726.
- [4] TANG, K. T., TOENNIES, J. P., and YIU, C. L., 1998, *Int. Rev. Phys. Chem.*, **17**, 363.
- [5] CAMBI, R., CAPPELLETTI, D., LIUTI, G., and PIRANI, F., 1991, *J. chem. Phys.*, **95**, 1852.
- [6] CAPPELLETTI, D., LIUTI, G., and PIRANI, F., 1991, *Chem. Phys. Lett.*, **183**, 297.
- [7] AQUILANTI, V., CAPPELLETTI, D., and PIRANI, F., 1996, *Chem. Phys.*, **209**, 299.
- [8] HERSCHBACH, D. R., 1966, *Adv. Chem. Phys.*, **10**, 319.
- [9] BROOKS, P. R., 1995, *Int. Rev. Phys. Chem.*, **14**, 327.
- [10] AQUILANTI, V., CANDORI, R., KUMAR, S. V. K., and PIRANI, F., 1995, *Chem. Phys. Lett.*, **237**, 456.
- [11] TOSI, P., DMITRIJEV, O., SOLDI, Y., BASSI, D., CAPPELLETTI, D., PIRANI, F., and AQUILANTI, V., 1993, *J. Chem. Phys.*, **99**, 985.
- [12] GILL, P. M. W., and RADOM, L., 1987, *Chem. Phys. Lett.*, **136**.
- [13] DABROWSKI, I., and HERZBERG, G., 1978, *J. Mol. Spectrosc.*, **73**, 183.
- [14] DEHMER, P., 1983, *Comments atom. molec. Phys.*, **13**, 205.
- [15] BRUNETTI, B., VECCHIOCATTIVI, F., AGUILAR-NAVARRO, A., and SOLÉ, A., 1986, *Chem. Phys. Lett.*, **126**, 245.
- [16] CARRINGTON, A., PYNE, C. H., and KNOWLES, P. J., 1995, *J. chem. Phys.*, **102**, 5979.
- [17] CARRINGTON, A., LEACH, C. A., MARR, A. J., SHAW, A. M., VIANT, M. R., HUTSON, J. M., and LAW, M. M., 1995, *J. chem. Phys.*, **102**, 2379.
- [18] CARRINGTON, A., PYNE, C. H., SHAW, A. M., TAYLOR, S. M., HUTSON, J. M., and LAW, M. M., 1996, *J. chem. Phys.*, **105**, 8602.
- [19] CASAVECCHIA, P., HE, G., SPARKS, R. K., and LEE, Y. T., 1981, *J. chem. Phys.*, **75**, 710.

- [20] CASAVECCHIA, P., HE, G., SPARKS, R.K., and LEE, Y.T., 1982, *J. chem. Phys.*, **77**, 1878.
- [21] AQUILANTI, V., CANDORI, R., and PIRANI, F., 1988, *J. chem. Phys.*, **89**, 6157.
- [22] AQUILANTI, V., CANDORI, R., MARIANI, L., PIRANI, F., and LIUTI, G., 1989 *J. phys. Chem.*, **93**, 130.
- [23] AQUILANTI, V., LUZZATTI, E., PIRANI, F., and VOLPI, G. G., 1988, *J. chem. Phys.*, **89**, 6165.
- [24] AQUILANTI, V., CANDORI, R., CAPPELLETTI, D., LUZZATTI, E., and PIRANI, F., 1990, *Chem. Phys.*, **145**, 29.
- [25] AQUILANTI, V., CAPPELLETTI, D., LORENT, V., and PIRANI, F., 1993, *J. phys. Chem.*, **97**, 2063.
- [26] AQUILANTI, V., ASCENZI, D., BRACA, E., CAPPELLETTI, D., and PIRANI, F., 2000, *Phys. Chem. Chem. Phys.*, in press.
- [27] AQUILANTI, V., CAPPELLETTI, D., and PIRANI, F., 1997, *Chem. Phys. Lett.*, **271**, 216.
- [28] AQUILANTI, V., CAPPELLETTI, D., and PIRANI, F., 1993, *J. chem. Soc. Faraday Trans.*, **89**, 1467.
- [29] HAY, P. J., WADT, W. R., and DUNNING JR., T. H., 1979, *Annu. Rev. Phys. Chem.*, **30**, 311.
- [30] TELLINGHUISEN, P. C., TELLINGHUISEN, J., COXON, J. A., VELAZCO, J. E., and SETSER, D. W., 1978, *J. chem. Phys.*, **68**, 5187.
- [31] MILLER, W. H., and MORGNER, H., 1977, *J. chem. Phys.*, **67**, 4923. See also BRUNETTI, B., and VECCHIOCATTIVI, F., 1993, *Cluster Ions*, edited by C. Ng, T. Baer and I. Powis (Chichester: Wiley), p. 359.
- [32] RAGONE, A. S., LEVY, D. H., and BERRY, R. S., 1982, *J. chem. Phys.*, **77**, 3784; SCHAEFER, S. H., BENDER, D., and TIEMANN, E., 1986, *Chem. Phys.*, **102**, 165.
- [33] MAGEE, J. L., 1940, *J. chem. Phys.*, **8**, 687.
- [34] OLSON, R. E., SMITH, F. T., and BAUER, E., 1971, *Appl. Optics*, **10**, 1848.
- [35] RAPP, D., and FRANCIS, W. E., 1962, *J. chem. Phys.*, **37**, 2631.
- [36] SMIRNOV, B. M., 1965, *Sov. Phys. Dokl.*, **10**, 218.
- [37] NIKITIN, E. E., REZNIKOV, A. I., and UMANSKII, S. Y., 1988, *Molec. Phys.*, **65**, 1301, and reference therein.
- [38] LIUTI, G., and PIRANI, F., 1985, *Chem. Phys. Lett.*, **122**, 245.
- [39] GOUGH, K. M., 1989, *J. chem. Phys.*, **91**, 2424; Ghanty, T. K., and GHOSH, S. K., 1996, *J. Phys. Chem.*, **100**, 17429.
- [40] AQUILANTI, V., and GROSSI, G., 1980, *J. chem. Phys.*, **73**, 1165.
- [41] AQUILANTI, V., CASAVECCHIA, P., GROSSI, G., and LAGANA, A., 1980, *J. chem. Phys.*, **73**, 1173.
- [42] AQUILANTI, V., LIUTI, G., PIRANI, F., and VECCHIOCATTIVI, F., 1989, *J. chem. Soc. Faraday Trans. 2*, **85**, 955.
- [43] AQUILANTI, V., CAVALLI, S., and GROSSI, G., 1996, *Z. Phys. D*, **36**, 1996.
- [44] DICK JR., B. G., and OVERHAUSER, A. W., 1958, *Phys. Rev.*, **112**, 90.
- [45] KRAUSS, M., 1977, *J. chem. Phys.*, **64**, 1712.
- [46] AQUILANTI, V., CAPPELLETTI, D., and PIRANI, F., 1997, *J. chem. Phys.*, **106**, 5043.
- [47] RADZIG, A. A., and SMIRNOV, B. M., 1985, *Reference Data on Atoms, Molecules and Ions* (Berlin: Springer Verlag).
- [48] BATES, D. R., and REID, H. G., 1968, *Adv. atom. molec. Phys.*, **4**, 13.
- [49] MILLER, T. M., and BEDERSON, B., 1977, *Adv. atom. molec. Phys.*, **13**, 1.
- [50] DUNHAM, J. L., 1932, *Phys. Rev.*, **41**, 721.
- [51] See for instance TOWNES, C. H., and SCHAWLOW, A. I., 1955, *Microwave Spectroscopy* (New York: McGraw Hill) p. 11.
- [52] GIANTURCO, F. A., and PATRIARCA, M., 1989, *Nuovo Cimento*, **11D**, 1287.
- [53] HUBER, K. P., and HERZBERG, G., 1979, *Molecular Spectra and Molecular Structure. IV. Constants of Diatomic Molecules*, (Princeton, NJ: van Nostrand).
- [54] WONG, M., BERNATH, P., and AMANO, T., 1982, *J. chem. Phys.*, **77**, 693.
- [55] JOHNS, J. W. C., 1984, *J. molec. Spectr.*, **106**, 124.